Ionization in H_2O – Bearing Carbon Dioxide Determined by Conductivity Measurements

Ryan Michael Capobianco

Thesis submitted to the faculty of the Virginia Polytechnic Institute and State University in partial fulfillment of the requirements for the degree of

Master of Science

In

Geosciences

Robert J. Bodnar
J. Donald Rimstidt
Miroslaw S. Gruszkiewicz

April 4th 2013
Blacksburg, Virginia

Keywords: carbon dioxide, corrosion, carbon capture and sequestration, enhanced geothermal energy, carbonic acid

Ionization in H_2O – Bearing Carbon Dioxide Determined by Conductivity Measurements

Ryan Michael Capobianco

ABSTRACT

Recent studies report rapid corrosion of metals and carbonation of minerals in contact with H_2O-saturated (or nearly saturated) CO_2. One explanation for this behavior is that addition of small amounts of H_2O to CO_2 leads to significant ionization within the fluid (analogous to corrosion in aqueous fluids). The extent of ionization in the bulk CO_2 fluid was determined using a flow-through conductivity cell capable of analyzing very dilute solutions. Experiments were conducted from 25 to 200°C and 25 to 200 bar with H_2O concentrations up to ~1650 ppmw. In all experiments, conductivities <10 nS/cm were obtained, indicating that the solution is essentially ion-free. This observation suggests that mobile ions are not present in the bulk CO_2–rich fluid, and that the observed corrosion and carbonation reactions are not the result of ionization in the bulk fluid.

ACKNOWLEDGMENTS

This thesis would not have been possible without the support of my committee members, Robert J. Bodnar, J. Donald Rimstidt and Miroslaw S. Gruszkiewicz. They have been very generous with their time and advice, both as pertains directly to this research project and to broader issues like effective scientific communication and the overall career direction.

Further, this thesis would not have been possible in a very literal sense without the help of David J. Wesolowski and the Geochemistry and Interfacial Sciences Group at Oak Ridge National Laboratory, where this research was conducted. My thanks also go out to Dave and all of the members of the Geochemistry group for countless productive conversations as I was interpreting data and working through experimental challenges.

My thanks go out to my current and former fellow graduate students in the Fluids Research Group, Rosario Espositio, Daniel Moncada, Matthew Steele-MacInnis, Pilar Lecumberri-Sanchez, Denise Levitan, Elizabeth Krukowski, Hector LaMadrid, and our visiting scholars. They have always been willing to take some time out of their day to field my many questions. In particular, Matthew Steele-MacInnis has been an amazing resource, providing insight into both scientific questions and professional development.

I would like to thank Elizabeth Krukowski and Kristie Dorfler for their support as I struggled to navigate both the many challenges unique to graduate school and the everyday challenges we all face. Elizabeth was always ready with encouragement, reassurance, an open ear, and if all else failed a cheesy movie to take my mind off things. Kristie brought her unique brand of enthusiasm which livens up even the most mundane challenges and has been a great sounding board.

Finally, I would like to thank my family. Without their constant support I would not have even been in a position to become a graduate student in the first place. I cannot begin to convey in these few words their patience, understanding, and the sacrifices they have made for me. A few years ago, I don't think any of us would have thought this would be possible. I can say with certainty that it still would not be without them.

This work was supported by the National Energy Technology Laboratory, Oak Ridge National Laboratory, and the National Science Foundation.

TABLE OF CONTENTS

LIST OF FIGURES

1. INTRODUCTION

The relationship between increasing atmospheric CO_2 levels and global climate change is well established (Intergovernmental Panel on Climate Change 2007). Capturing CO_2 from point emission sources such as coal-fired power plants and cement manufacturing facilities and injecting it into confined geologic formations (carbon capture and storage, or CCS) is one means to reduce the atmospheric impact of fossil fuel combustion. This approach has the potential to store CO_2 for hundreds (or thousands) of years (Benson and Cole 2008). Another option to reduce CO_2 emissions is to increase production from alternative energy sources, such as geothermal energy, that do not generate CO_2 during electricity production. Moreover, using CO_2 produced by burning of fossil fuels as the working fluid in enhanced geothermal energy production has the potential to avoid complications associated with H_2O working fluids. These complications include dissolution/precipitation of minerals in the reservoir and scaling in the pipes and turbines (Pruess 2006). Additional advantages of using CO_2 in enhanced geothermal energy production include its high expansivity, low viscosity, and elimination of the necessity of having an adequate supply of water (Pruess 2006).

Using CO_2 as the working fluid in geothermal energy production or storing CO_2 in geologic formations may result in alteration of the host formation, which will initially be filled with aqueous solutions such as brines. Injection of CO_2 may lead to mineral dissolution, precipitation, or in-place phase changes as the fluids and minerals equilibrate. Precipitation of mineral phases or reactions leading to formation of carbonate minerals ("carbonation") may enhance storage security (Gaus, Azaroual et al. 2005) by filling existing or newly created fractures in the caprock. Conversely, elimination of fractures in the reservoir may reduce the

permeability of the formation, which would negatively impact geothermal energy extraction. Similarly, dissolution of mineral phases may increase permeability but decrease storage security, especially if dissolution occurs in the cap rock above the storage formation (Pruess 2006). In addition, water-bearing CO_2 could promote corrosion of metals and other materials used in these industrial processes, requiring more frequent maintenance and/or replacement (McGrail, Schaef et al. 2009).

Until recently, reactions occurring in geological reservoirs associated with CCS have focused on CO_2-saturated brine – mineral interactions (Gaus 2010). However, because the CO_2-rich phase is less dense than the aqueous phase under PT conditions relevant to CCS, following injection the CO_2 will migrate to the top of the formation where it will be in contact with cap rock (in saturated conditions, the aqueous phase will be present as a wetting fluid). Likewise, the CO_2-rich phase will be in contact with metal during CCS injection and when CO_2 is the working fluid in geothermal energy production. If the bulk CO_2-rich phase (and/or the wetting phase) has a high reactivity, it could have a significant impact on equipment corrosion and reservoir security.

The formation and ionization of carbonic acid can lead to dissolution and/or carbonization of materials in contact with the solution. The interaction of H_2O and CO_2 when CO_2 is the solvent (i.e., in very CO_2-rich compositions) and the mechanism behind the rapid carbonization reactions reported in previous studies is not well understood. Possibilities include: formation and ionization of carbonic acid in the bulk CO_2 solution (Figure 1A); ionization occurring only near solid surfaces, such as in a thin film of H_2O or a relatively H_2O-enriched region (Figure 1B) as suggested by Lin et al. (2008); direct interaction of molecular H_2O and CO_2 with the surface as described by Schaef et al. (2011) for brucite; or some combination of the

above. In an effort to better understand this process, the electrical conductivity of water-bearing CO_2 has been measured in order to examine the ionization of H_2CO_3 in very CO_2-rich fluids.

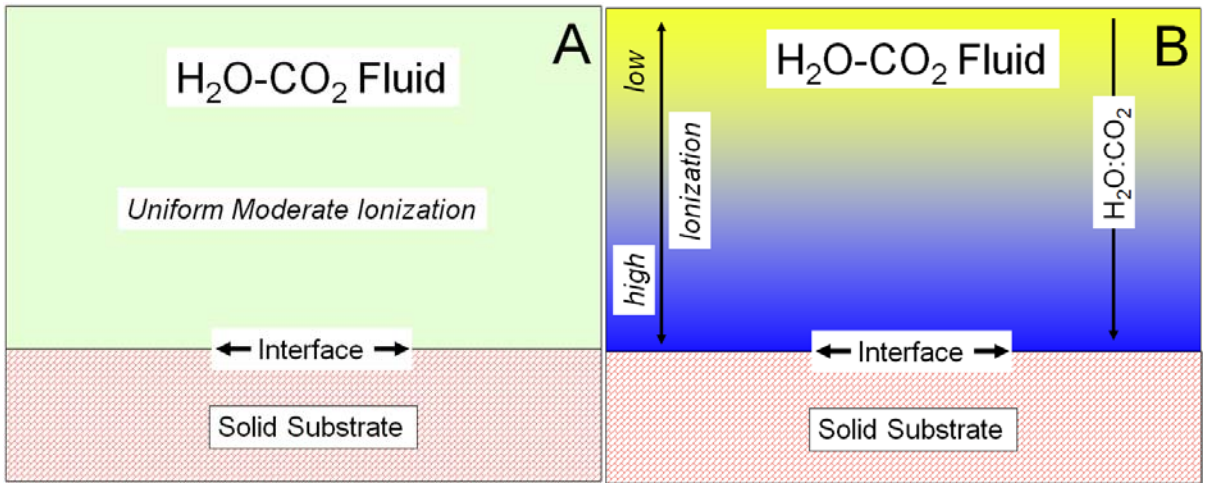

Figure 1. Two end-member scenarios for ionization in CO_2 – rich, H_2O – CO_2 solutions. In scenario A, ionization occurs in the bulk fluid and is relatively uniform throughout. In scenario B, ionization is concentrated near the mineral or metal surface, such as in a thin film of H_2O – rich fluid. In a third scenario, not depicted, ionization does not occur. In this scenario, carbonation reactions occur due to direct interaction of CO_2 with the surface.

2. MATERIALS AND METHODS

Data reported here were obtained using a flow-through conductivity technique which is ideal for studying ionization in low-conductivity fluids. The instrument used in this experiment is a modified version of a previously described design (Zimmerman 1994; Zimmerman, Gruszkiewicz et al. 1995). The instrument is shown schematically in Fig. 2 and is described in detail below.

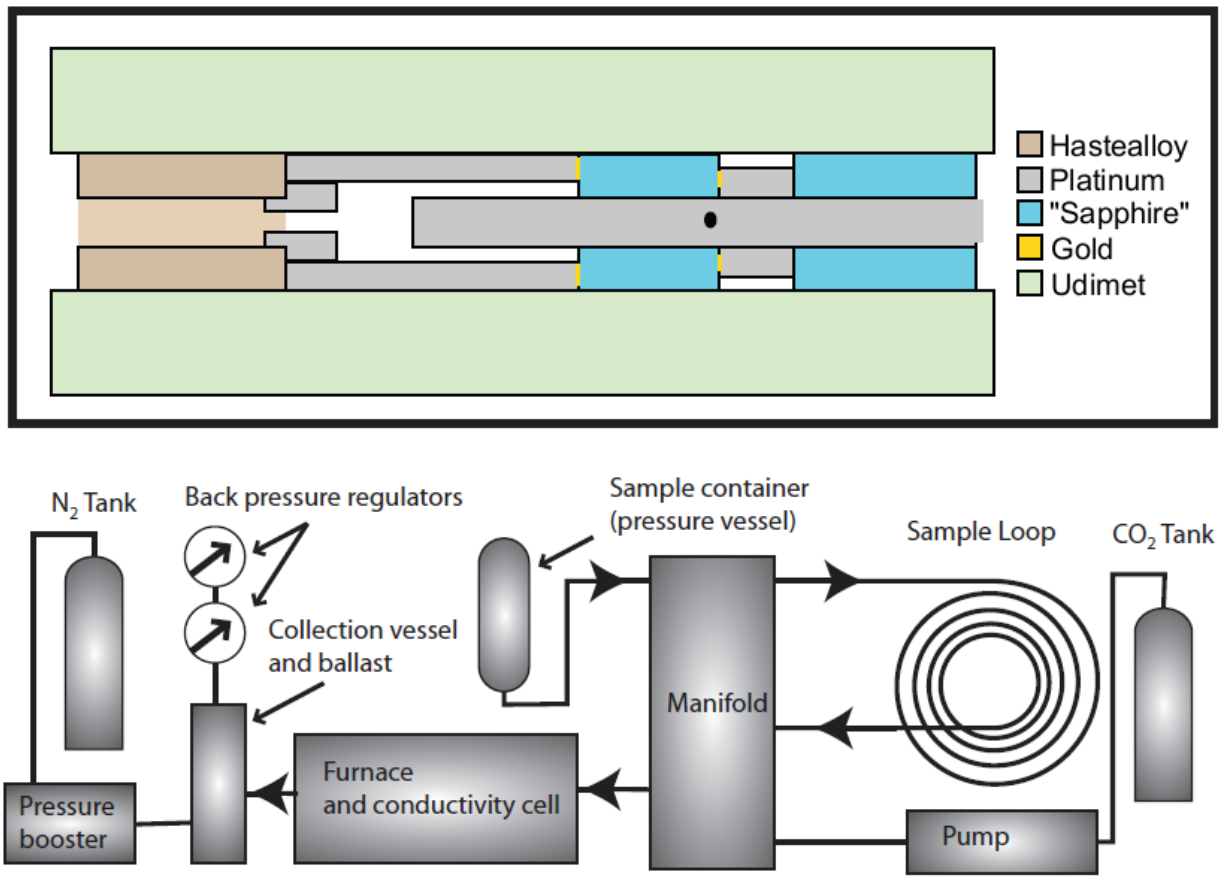

Figure 2. Schematic diagram of the conductance cell and of the entire apparatus. Top: Schematic cut-away view of the interior of the conductance cell. The Udimet pressure vessel and all tubing and rods extend beyond the area depicted. The internal diameter of the Udimet vessel is 0.635 cm.
Bottom: Schematic diagram of the entire conductance apparatus, including the sample loop, pumps, furnace, gas sources and measuring devices. The sample flow path is indicated by the large arrows.

2.1 Conductivity Measurements

When a voltage is applied to a fluid containing dissolved ions, there is a tendency for ions to move toward their opposing charge. The ions act as charge carriers, allowing the solution to conduct electricity. The units of conductance are siemens (*S*), which are reciprocal ohms (Ω) such that:

$$S = 1/\Omega = A/V \qquad (1)$$

where A is the current in amperes, and V is the voltage in volts. The conductance of the solution depends on the concentration and mobility of free ions, the geometry of the conductance cell, and other effects (Justice 1983). A more useful quantity when comparing results between experiments is the specific conductance or conductivity of the solution, which is the conductance per centimeter (S/cm) defined as the conductance of a solution enclosed between 1 cm x 1 cm electrodes spaced 1 cm apart.

Flow-through conductivity is a technique for studying ionization in low-conductivity fluids such as dilute or low-density solutions. This approach reduces errors caused by sorption to the walls of the cell and accumulation of impurities compared to a static cell. The instrument used in this experiment is a modified version of a previously described design (Zimmerman 1994; Zimmerman, Gruszkiewicz et al. 1995), as described below. The original instrument was designed for aqueous fluids and is capable of reaching 1 kbar and 750°C. Due to the high compressibility of carbon dioxide, the loading procedure was modified, as described in section below, which currently limits the maximum experimental pressure for CO_2 – rich fluids to ~200 bars.

2.2 Instrument Design

The design used in this study is shown schematically in Fig. 2 (bottom). A computer-controlled pump (DBR-JEFRI Equipment PMP-0160-1-20-MB-400-M3-C4) is charged with CO_2 (Airgas certified 99.999% CO_2 with < 3 ppmw H_2O) directly from the tank. The fluid is brought to experimental pressure, and then pumped at a constant rate of 0.4 cc/min through 1/8" (0.318 cm) Hastelloy tubing (all Hastelloy used in this experiment is Hastelloy C276) into and through the cell. The fluid exits the cell into a collection chamber (which also serves as one of two pressure ballasts) and is externally chilled with $CO_{2(s)}$ (dry ice) at -78°C.

Pressure inside the conductance cell is balanced by N_2 in the space between the cell and the pressure vessel. Nitrogen pressure is generated by a pressure booster (Haskel International) operated by compressed air, and is maintained by two back-pressure regulators (BPR). The collection chamber and additional ballast provide excess volume to reduce the pressure response of the system as the volume of the collected waste solution increases, and to small perturbations caused, for example, by switching between the sample and the pump fluid. Pressure is measured by a pressure transducer (Precise Sensors 6550-1379-G-360-15F-B10-10). Experimental pressure was typically controlled to ± 0.1 bar, and never exceeded ± 0.3 bar, with the exception of two experiments (at 200 bar and 25°C, and at 150 bar and 35°C) when the BPR stuck in the open position momentarily, resulting in a brief pressure drop of ~2 bar. These irregularities occurred between measurements and pressure returned to the normal range before the next measurement was taken. Near the end of the series of experiments, a leak developed through an inaccessible seal in the collection vessel. This necessitated continual addition of N_2 to balance outflow, and the BPRs were closed.

The cell is heated by an electric furnace (Applied Test Systems, Inc Series 3210). The heating element surrounding the cell is controlled by a Barber-Colman CIMAC 2 controller via an Instrulab 4212A temperature monitor. Cell temperature is measured by two platinum resistance probes calibrated to NIST-traceable fixed-point standards and accurate to ± 0.02 K over the temperature range of the experiments. Thermocouples are used to individually control two additional heating elements within the furnace: a pre- and a post-heater. The pre- and post-heaters were only used in experiments conducted at or above 100°C. Temperature was typically controlled to ± 0.02°C. In three experiments (at 25°C 150 bar; at 150°C 200 bar; and at 150°C 150 bar) temperature fluctuations of up to ± 0.29°C occurred. There was little to no discernible impact on measured resistances.

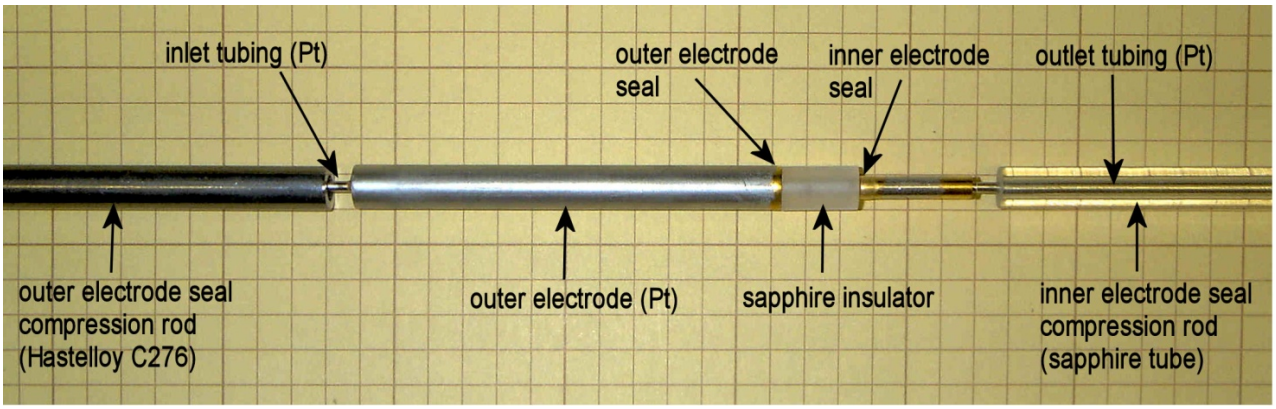

Figure 3. Photograph of the conductance cell, prior to assembly. Each square is 5 by 5 mm.

The conductance cell, shown schematically in Figure 2 and in a photograph in Figure 3, consists of a 6.22 cm length of ¼" (0.635 cm) outer diameter (OD), 0.180" (0.457 cm) inner diameter (ID), platinum tubing ("the cup") which is gold-soldered to the 1/16" (0.159 cm) Pt inflow tubing. The cup is compressed into a gold seal that is annealed to a 1.1 cm long, 1/4" (0.635 cm) OD sapphire cylinder with a 1/16" (0.159 cm) hole drilled along its long axis. A second gold seal is annealed to the opposite end of the sapphire cylinder, which is compressed

into platinum to seal the outflow side of the cell. The inner electrode consists of 1/16” (0.159 cm) platinum tubing that also serves as the outflow tubing. The platinum tubing passes through the sapphire insulator and protrudes 5.15 cm into the cup. The inner electrode is welded shut on the protruding end. Solution exits the cell through holes at the base of the inner electrode. The inner and outer electrodes are platinized (coated in platinum black).

The cell is lightly compressed by a Hastelloy rod on the inflow side and a sapphire rod on the outflow side. The sapphire rod serves as an electrical insulator between the inner and outer electrodes. The entire cell assembly is contained within a ¼” (0.635cm) internal diameter, 1.5” (3.81 cm) outer diameter pressure vessel made of Udimet 720 superalloy. There is a slight gap between the conductance cell assembly and the Udimet pressure vessel. The space outside the conductance cell is pressurized with N_2 to balance the inflow pressure such that the pressure gradient across the cell walls is minimized. This reduces the force needed to compress the gold seals between the sapphire and platinum. The gold seals are compressed by a series of two threaded bolts, Bellville springs, and washers.

The sample is contained in a loop of Hastelloy tubing with ~15 cc internal volume. The sample loop can be isolated from the rest of the apparatus (switched in or out of the line of flow) by means of a manifold consisting of several Hastelloy valves and 1/8” OD tubing. Switching the loop in and out requires flow to be stopped briefly. The tubing between the loop and the conductance cell has ~2 cc internal volume, so after each sample injection the typical experiment records a baseline (< 3 ppmw H_2O in CO_2) for 2 cc (5 min), the sample for ~15 cc (~38 min) and then a baseline again. Resistance results from a typical experiment are presented in Figure 4. The shaded regions on this figure indicate values that are below the estimated limit of quantification (resistance is reciprocal conductivity, so higher resistance values represent lower signal).

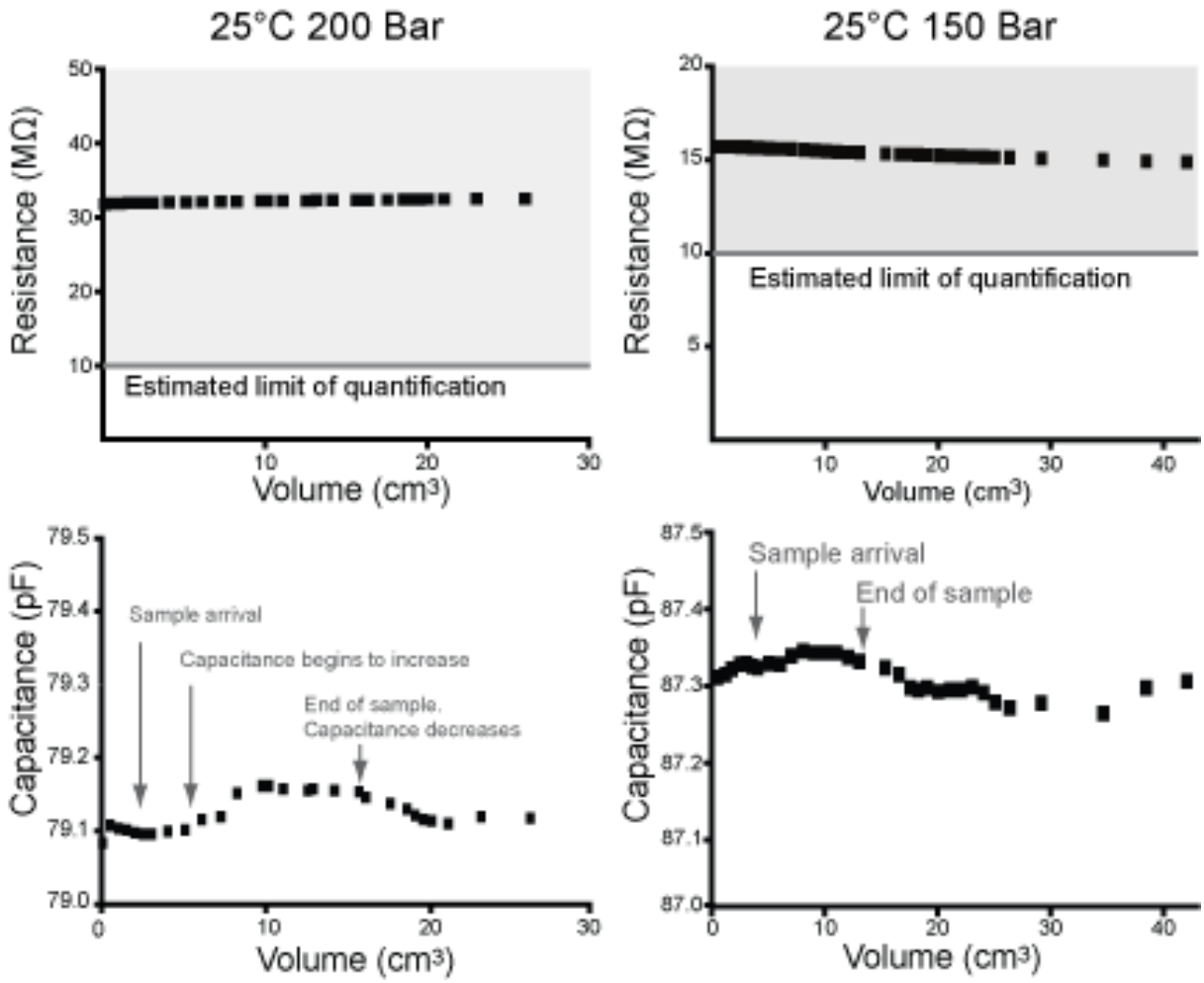

Figure 4. Typical unprocessed resistance and capacitance results illustrating the typical trends observed. The shaded regions above the line labeled "estimated limit of quantification" are values *below* the estimated limit of quantification (resistance is reciprocal conductivity). In all figures the volumes from 0 to ~2 cm^3 and > ~17cm^3 represent "dry" (< 3ppmw H_2O) CO_2). The portion of the plot corresponding to H_2O-bearing CO_2 (wet) is from ~2 - ~17cm^3. In all experiments, there was no detectable difference between the resistance of "dry" and "wet" CO_2. In some experiments, such as at 25 °C and 200 bars, there is a small detectable change in capacitance which lags the sample signal. In others, such as 25°C and 150 bars, the change may be present but is less clear.

2.3 Determination of the cell constant

The cell constant, which relates the measured cell resistance (Ω) to the resistivity of the solution (Ω/cm), can be calculated from the geometry of the cell. For this apparatus, the calculated cell constant is 0.0327/cm. However, factors such as electrical fringing effects can result in a true cell constant that differs from the calculated constant, so it is necessary to calibrate the cell using solutions of known conductivity.

The cell was calibrated at 25°C using commercially available 0.00017 M and 0.00068 M Alfa Aesar conductivity standards and custom prepared KCl solutions. Solutions were prepared gravimetrically using 18.3 MΩ water (conductivity water) and ≥99.95% pure KCl (Baker ACS reagent) that was additionally purified by filtering and double crystallization from conductivity water. The final concentration of non-KCl components was not verified. Solutions were prepared at target molarities of 0.0001 M, 0.001 M, 0.005 M, 0.01 M, 0.025 M and 0.05 M. The conductivities of these solutions were calculated after Justice (1983). Solutions were prepared and introduced into the sample loop in the manner described by Zimmerman (1994) (in section 2.4 “Experimental Method”).

A total of 14 calibration runs were made, including duplicate runs for some solutions, for a total of eight unique molalities tested. For each solution, the cell constant was calculated by:

$$k = R_x \kappa \tag{3}$$

where k is the cell constant, R_x is the resistance of the solution, and κ is specific conductivity of the solution.

Ion interactions such as ion pairing, which increase with increasing molality, will result in inaccuracy at any concentration greater than infinite dilution. When ion pairing occurs, the

paired ions (in this case KCl^0) are neutral and do not contribute to solution conductivity. The ion pairing effect is minimized in very dilute solutions. Conversely, however, very dilute solutions are sensitive to any contamination or sorption effects. The apparent cell constant was calculated at multiple molalities and then extrapolated to infinite dilution by linear regression. It was found that all results from custom prepared solutions except the most dilute solution agreed well with linear extrapolation (R^2 of 0.946) to infinite dilution. The apparent cell constant determined from the most dilute solution was rejected as an outlier, for reasons described above. This approach calculated a cell constant of 0.0298/cm. Commercial solutions were not included in this calculation because it was not possible to degas these solutions without altering the concentration of KCl in the solution. Degassing the solutions is necessary to remove atmospheric CO_2 and O_2, which ionize and can introduce error. However, the commercial solutions were in general agreement (+/- 2 to 6%) with the cell constant as determined above.

After the cell constant was determined, the cell apparatus was flushed with degassed conductivity water for about two weeks to remove residual KCl. We were unable to register a resistance reading consistent with the resistivity of conductivity water (18.3 MΩ), leading us to suspect that KCl (or other impurities) was still desorbing from the interior of the apparatus. We could not rule out the possibility that water vapor diffused through the N_2 and condensed outside of the cell. Condensation or sorption of water on the outside wall of the cell would result in some current passing through the condensed water which could account for the higher conductivity. We added the cold trap described above to minimize this effect in subsequent experiments. The apparent conductivity of conductivity water was ~1 mS/cm at 1 kHz, or ~0.7% of the conductivity of the most dilute solution used for calibration. This may have introduced a small

amount of unconstrained error, so we report the cell constant as 0.030/cm (rather than 0.0298/cm) and use this value in subsequent calculations.

2.4 Sample preparation and loading

In this experiment, two pressure vessels were used to prepare H_2O-bearing, CO_2-rich solutions to be introduced into the sample loop. The first is a titanium vessel with an internal volume of ~60 cm^3. This vessel was used for experiments up to 80 bar. The second is a steel vessel (Swagelok) with an internal volume of 300 cm^3. This vessel was used for all other experiments. Vessels and syringes used in this experiment were thoroughly rinsed at least three times in 18.3 MΩ conductivity water and then desiccated overnight prior to each use. The steel vessel had not been used in prior experiments, so it was additionally rinsed in methanol to remove possible contaminants from the manufacturing process.

The pressure vessel was filled with argon to exclude atmospheric gases. A syringe was filled with conductivity water and weighed on a balance accurate to 0.1 mg. The water was injected into the pressure vessel, and the syringe was weighed again to determine the mass of H_2O that had been injected. Balances used in this experiment were routinely calibrated against external mass standards and showed negligible drift. In experiments run at saturation, excess H_2O was used (~4 times saturation at the desired pressure and at room temperature). The vessel was then sealed and the mass was recorded.

The vessel was placed in a Dewar filled with crushed dry ice and chilled for 15 minutes. While still chilled in the Dewar, the vessel was evacuated until the pressure was less than 100 mTorr (~0.00013 bar). This procedure removed the argon from the vessel while minimizing H_2O

loss to sublimation. The vessel was then removed from the Dewar and pressurized with CO_2 (Airgas certified 99.999% CO_2 with < 1 ppmw H_2O). The titanium vessel was pressurized to ~200 bar and the steel vessel was pressurized to ~300 bar. Heating due to pressurization and prior to chilling of the vessel resulted in the top half being at higher temperature than the lower half. The vessel was allowed to thermally equilibrate for about 30 minutes while pressure was monitored. When thermal equilibration resulted in a pressure change, the pressure change was always negative. In this case, additional CO_2 was added to the vessel and it was again allowed to equilibrate. Equilibration did not result in pressure increase, which would have required CO_2 to be released. As a result flow was always one-way into the vessel. The mass of the filled vessel was recorded after the required pressure and temperature were achieved as described above.

The sample loop was isolated from the apparatus and evacuated prior to filling. After the loop was evacuated, it was sealed and the pressure vessel was connected to the manifold. The sample was allowed to expand into the sample loop. This resulted in perceptible cooling, so the sample vessel was gently heated until it was slightly warm to the touch. The loading procedure lasted about 15 minutes. The sample loop itself was at ambient conditions (about 22°C). The maximum amount of H_2O introduced into the sample loop was limited to that amount required to achieve saturation at room temperature and 300 bars, or about 1600 ppmw. When using the 300cc steel pressure vessel, three experiments were run with one sample charge, resulting in lower pressure in the sample vessel on each filling.

Prior to and throughout the loading procedure, the cell was flushed with "dry" CO_2 at experimental temperature and pressure bypassing the loop. After the sample was loaded into the loop, the bypass was cut off, briefly stopping flow. The loop was opened to the pump and, if necessary, was compressed to bring it to experimental pressure. The sample was typically

compressed less than 0.5 cm^3. The loop was then opened to the cell and flow was resumed. The entire procedure, from stopping to resuming flow, took less than a minute.

2.5 Experimental procedure

The flow rate during the experiment was 0.4 cm^3 per minute. Throughout the experiment the resistance and capacitance of the solution were measured by a Wayne Kerr Precision Component Analyzer 6425B, assuming an equivalent circuit of a capacitor and resistor in parallel. These data were recorded before, during, and after the experiment. Conductivity measurements become less accurate at high frequencies, as current passing through the capacitative component of the equivalent circuit begins to dominate (Bockris, Reddy et al. 2000). At low frequency, polarization of the electrodes results in concentration gradients in the solution. Therefore, conductivity values are measured at multiple frequencies and then extrapolated to infinite frequency. When a plateau was reached in the resistance reading (or near the end of sample volume, ~15cc depending on how much the loop was compressed) the resistance was recorded at 1, 2, 5, 10, and 20 kHz. In many experiments, measurements at 10 and 20 kHz resulted in anomalous readings, including negative resistance. For consistency, extrapolations to infinite frequency only used the resistance readings at 1, 2, and 5 kHz for all experiments. We found a linear relationship between conductivity at 1kHz and conductivity extrapolated to infinite frequency for $H_2O - CO_2$ solutions with ~1200-1600 ppmw H_2O ($R^2 = 0.95$). When data at 2, and 5 kHz were not useable or not available, this linear relationship is used to estimate conductivity at infinite frequency.

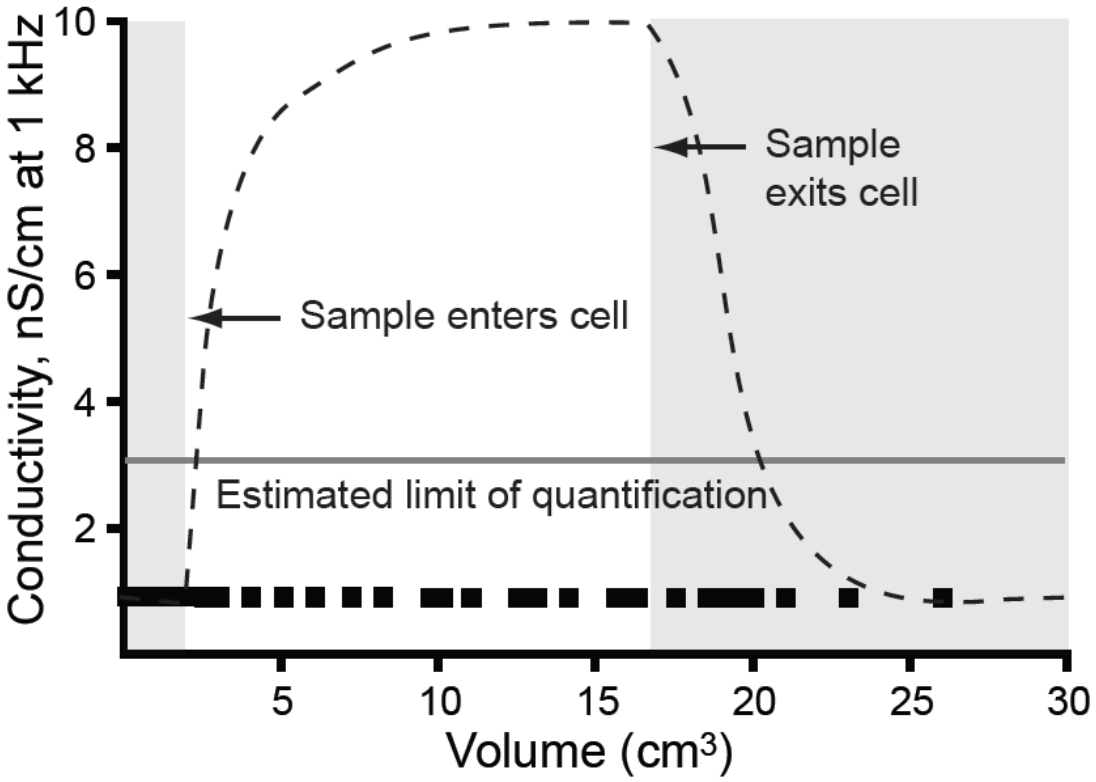

Figure 5. Typical conductivity results from experiments in this study conducted at 1 kHz. The shaded region represents flow of "dry" (< 3ppmw H_2O) CO_2 through the cell. The unshaded region represents the sample, in this case CO_2 containing ~1550 ppmw H_2O. The grey line is the estimated limit of quantification. There is no detectable difference between the sample and "dry" CO_2, and all values are below the estimated limit of quantification. Note that the limit of quantification at 1 kHz (3.0 nS/cm) is lower than in other figures because those data are reported at infinite frequency.

The conductivity of a fluid, κ, is related to the measured resistance, R, and the cell constant, k by:

$$\kappa = k/R \tag{3}$$

Figure 5 depicts the same resistance data presented in the upper left panel in Figure 4 (25°C, 200 bar), after conversion to conductivity by Equation 1. Note that conductivities in Figure 5 are at 1 kHz (not extrapolated to infinite frequency). During the experiment, "dry" CO_2 is continuously flushed through the cell, and intermittently a slug of wet CO_2 (the sample) is introduced. Introducing the sample requires a brief stoppage of flow. In an idealized flow conductance

experiment, Figure 3 would show rapid change in conductivity when the wet CO_2 sample reaches the cell (at ~2 cm^3), and the conductivity would plateau at the true value before all of the sample has passed through the cell (at ~17 cm^3), as shown schematically in Figure 5. Development of a plateau in the conductivity data is a result of sweeping out the blank by the sample (with limited mixing at the front of the sample plug) and progressive sorption of solute to the cell and tubing, eventually reaching equilibrium. This expected idealized pattern was not observed in our experiments, suggesting that there was no significant difference in concentration of ionized species between "wet" and "dry" CO_2. As no distinguishable plateau was observed, the conductivity values reported here are the values measured near the end of the period over which the sample is in the cell. All solution conductivity values reported are below the estimated limit of quantification, i.e., the conductivities were extremely low.

3. RESULTS

In all cases, except where contamination was suspected (immediately following the replacement of an O-ring in the sample vessel), no significant difference in resistance was observed between the H_2O – CO_2 sample and "dry" CO_2 from the CO_2 supply tank, and all resistance readings of CO_2 solutions were below the estimated limit of quantification. Small changes in capacitance were typically, but not always, associated with or slightly lagged behind the arrival of the sample. Examples of typical unprocessed capacitance and resistance data from experiments are shown in Figure 4.

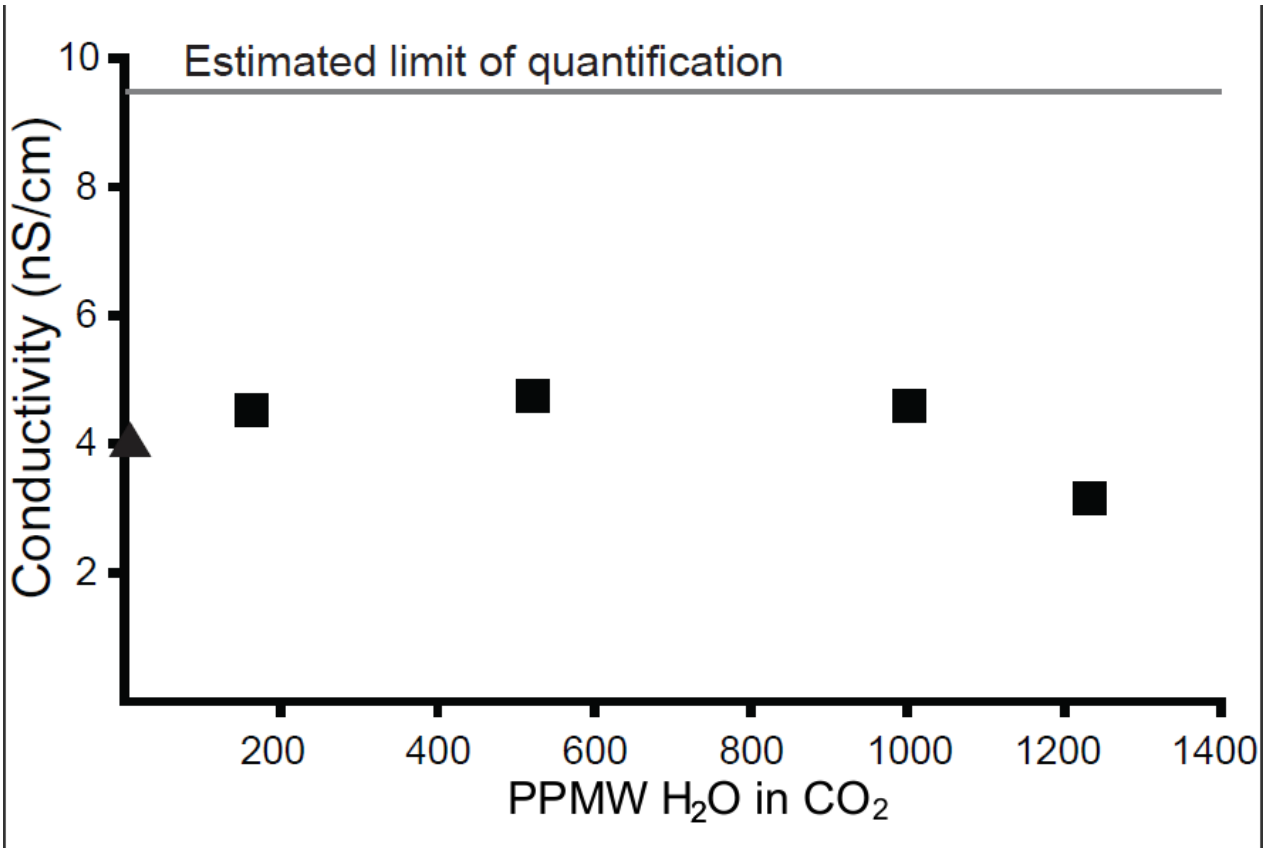

Figure 6. Conductivity at infinite frequency of CO_2 solutions with H_2O concentrations from <3 ppmw (plotted at 1) to saturation at 25°C and 80 bar. The solid triangle indicates the average of 12 measurements of CO_2 standards made at these conditions. Eleven of those measurements are from blanks that were run before and after experimental solutions. Note that all values are below the estimated limit of quantification (indicated by the grey line).

All concentrations of H_2O in CO_2 from <3 ppmw (plotted at 1 ppmw in Figure 6) to saturation were found to have maximum conductivity < ~5 nS/cm at 25°C, 80 bar. No systematic relationship was found between the concentration of H_2O in CO_2 and conductivity at 25°C and 80 bar, as illustrated in Figure 6, nor was there a detectable difference between the H_2O – CO_2 solution and the "dry" (<3 ppmw H_2O) tank CO_2. Other PT conditions, from near critical (31°C and 73.9 bar) to 200°C, 200 bar were tested at the maximum H_2O concentration which could be introduced, ~1650 ppmw H_2O. The solution conductivity did not exceed 10 nS/cm in any of the experiments, as shown in Figure 7. The conductivity of paper is presented as a point of reference on Figure 5 to illustrate the very low conductivities of these fluids.

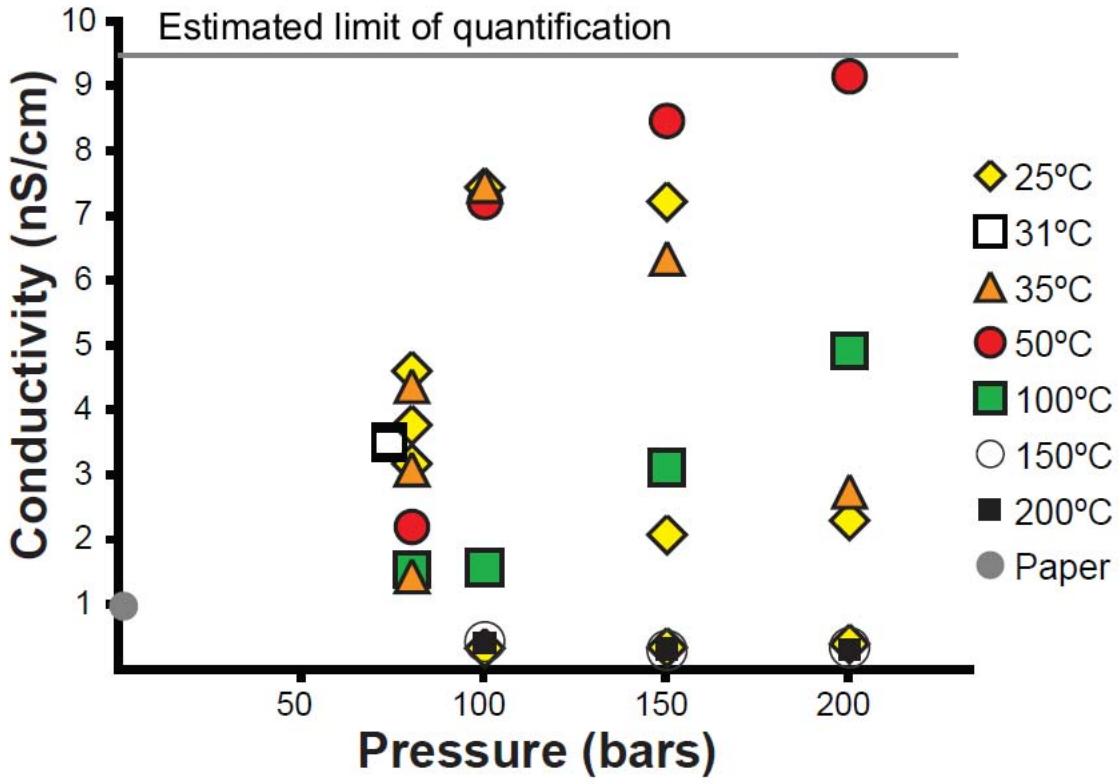

Figure 7. Conductivity at infinite frequency of CO_2 with ~1600 ppmw H_2O. At 25°C, CO_2 is H_2O-saturated, (~1250 ppmw H_2O). In the higher temperature experiments the CO_2 is undersaturated, and contains ~1600 ppmw H_2O. The conductivity of paper is provided as a point of reference, plotted at 1 bar. All values are below the estimated limit of quantification.

4. DISCUSSION

4.1 Experimental results in comparison to common solutions

For all PT conditions and concentrations of H_2O tested, the maximum conductivity of H_2O – CO_2 solutions is very low (< 10 nS at infinite frequency), comparable to an insulator such as paper which has a conductivity of ~1 nS/cm (Fig. 7). The conductivity of tested CO_2 solutions at 25°C and 80 bar, a KCl solution used in cell calibration, and typical values for sea water, distilled water, and completely deionized (18.3 MΩ) water are shown in Figure 8. Conductivity values range from that of a good conductor (sea water) to that of an insulator (18.3 MΩ water). To put this into perspective, conductivity in deionized water is due only to auto-ionization of water, which produces an equilibrium concentration of 10^{-7} moles per liter of both H_3O^+ and OH^-. All tested H_2O - CO_2 solutions have conductivity at least one order of magnitude *less* than 18.3 MΩ water. This illustrates the very low ionic concentrations in these fluids.

4.2 Estimated limit of quantification

A statistical approach (10 times the standard deviation across multiple experiments, n=12) for CO_2 with <3 ppmw H_2O at 25°C and 80 bar was used to estimate a limit of quantification of 41 MΩ at 1 kHz. With a cell constant of 0.03/cm, this translates to 0.73 nS/cm at 1 kHz. Using an approximately linear relationship between conductivity at 1 kHz and conductivity at infinite frequency (see electronic annex) we can calculate a limit of quantification of about 2.6 nS/cm at infinite frequency. However, we feel a more conservative estimate of the

limit of quantification is necessary due to certain obstacles inherent in measurements of these exceptionally dilute solutions, as explained in section 3.3. We estimate a conservative limit of quantification of 10 MΩ at 1 kHz, equivalent to 3.0 nS/cm at 1 kHz or ~9.5 nS/cm at infinite frequency.

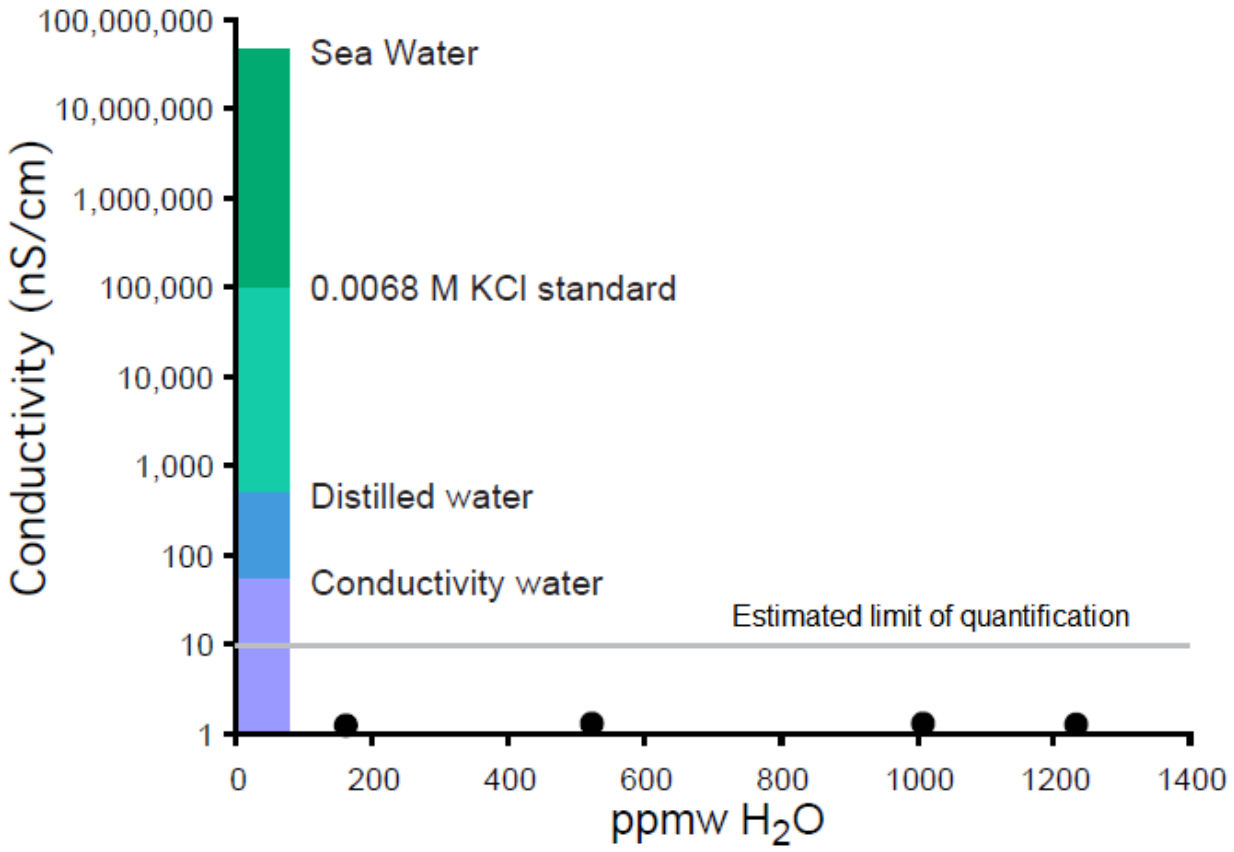

Figure 8. Conductivity of H_2O – bearing CO_2 at 1 kHz compared to conductivities of other common solutions. Compositions along the x-axis only apply to the CO_2 solutions of this study. The CO_2 solutions represent the same data as shown on Figure 6. The 0.00068M KCl solution is a standard used in cell calibration. Other representative solutions are shown only for comparison.

4.3 Conductivity experiments with very dilute solutions

The main factors affecting our estimation of the limit of quantification are the nature of conductivity measurements and the size of the cell. The cell is approximated by an equivalent circuit of a resistor and capacitor in parallel. To the extent that this approximation is correct, a portion of the total current (and hence apparent conductivity) is due to charging and discharging of the electrodes as the current alternates, analogous to a capacitor, and a portion of the total current flows through the solution as ions move in response to the applied voltage, analogous to a resistor.

The portion of the total current attributed to the capacitive component is determined based on the phase shift between the alternating voltage and current. If all of the current flows through the resistive leg of the circuit (i.e., the conductivity of the solution is large relative to the capacitance), there will be no phase shift. If all of the current flows through the capacitive leg of the circuit (the solution has no conductivity), the phase shift will be 90°. We found that, at the frequencies used in these experiments, the phase shift angle was nearly 90°, indicating that the conductivity of the solution is essentially nil and that most of the current was due to the capacitive leg of the circuit. Therefore, a small error in determining the capacitance could induce disproportionate error in conductance attributed to the solution. Secondly, the cell used in this study was designed for dilute and low-density aqueous solutions. The cell constant is small (0.030/cm) which makes it possible to measure fluids exhibiting low ionization. It was found that the solutions measured in this experiment have conductivities about 20 times *less* than 18.3 MΩ conductivity water. The ideal cell constant for such low conductivities is smaller than the cell constant of the present apparatus, ~0.0005/cm or smaller. To achieve such a cell constant would

require large, closely spaced electrodes. A design such as this would show larger adsorption per unit volume, as well as higher capacitance.

As with any experiment measuring conductivity of fluids with extremely low conductance, exceptional cleanliness is essential. Conductivity on the order of nS/cm, as routinely measured in this experiment, is comparable to the conductivity of nano-molal concentrations of KCl in aqueous solution (after correcting for the much larger conductivity due to the auto-ionization of water) at 25°C and 1 bar. The results for an aqueous KCl solution are not directly applicable to the present study because the conductivity due to the same concentration of KCl in CO_2 would be different (were it possible to dissolve this quantity of KCl in CO_2), owing to the different physical properties of CO_2 compared to water at 25°C and 1 bar. However, the example above for an aqueous system can be used as a convenient point of reference when considering the present results in CO_2 – rich solutions. In solutions with low conductivity, small quantities of ionic contaminants will have a large effect on the conductivity of the fluid. Ions may be desorbed from the sample container or tubing in the apparatus, retained in dead space, or acquired from some other source.

Over the course of these experiments we observed an overall tendency to higher resistance with elapsed experiment time, which is consistent with gradual removal of some small amount of impurity. When CO_2 was first introduced into the apparatus, "Dry" (< 3 ppmw H_2O) CO_2 had a conductivity (3.2 nS/cm at 1 kHz) ~2.5 times larger than that of the same CO_2 sample measured on the second day (1.3 nS/cm at 1kHz), when the conductivity reached approximately a plateau. The conductivity of this same CO_2 sample had decreased by a factor of one hundred by after 30 days to ~12 pS/cm at 1 kHz. The trend toward lower conductivity with time suggests

that some trace amounts of CO_2 – soluble ionized contaminants were gradually removed from the system.

In some experiments, resistance values of 2.2 to 2.3GΩ (~14 to ~13 pS/cm) were recorded at 1 kHz. These results are significantly below the estimated limit of quantification, so there is a high degree of uncertainty in these values. Below the estimated limit of quantification, factors such as changes in humidity and EM induction prevent meaningful comparison between experiments run on different days, or even different times in the same day. However, within a given experiment, a relative change in the concentration of ions between "dry" and "wet" CO_2 would be detectable well below the estimated limit of quantification. Over the PTX range tested, all values were below the estimated limit of quantification, and no significant difference between "dry" and "wet" CO_2 was detected.

4.4 Relationship between water availability and the formation and ionization of carbonic acid

Recent studies (Lin, Fujii et al. 2008; McGrail, Schaef et al. 2009; Regnault, Lagneau et al. 2009; Schaef, Windisch Jr et al. 2011) have investigated the reactivity of "wet" CO_2 with geological and man-made materials. These studies agree that H_2O-saturated (or near saturated) CO_2 promotes carbonation reactions that are not observed to occur in "dry" CO_2. Studies which also tested CO_2-saturated H_2O (Lin, Fujii et al. 2008; McGrail, Schaef et al. 2009) present evidence that carbonation reactions proceed more rapidly in contact with the CO_2-rich phase, compared to when the substrate is in contact with the aqueous phase.

In aqueous solutions, CO_2 and H_2O react to form carbonic acid:

$$CO_2 + H_2O = H_2CO_3 \quad (4)$$

Some carbonic acid subsequently dissociates or ionizes:

$$H_2CO_3 = H^+ + HCO_3^- \quad (5)$$

Equation 5 follows the convention of using H^+ to denote the hydronium ion (H_3O^+). In aqueous solutions we assume that there is excess H_2O so this notion is appropriate, but we cannot make this assumption for CO_2-rich solutions. A more complete way to express (5) is:

$$H_2CO_3 + H_2O = H_3O^+ + HCO_3^- \quad (6)$$

So the full reaction, from neutral species to products, is:

$$2H_2O + CO_2 = H_3O^+ + HCO_3^- \quad (7)$$

It is likely that reaction of H_2CO_3 with OH^- (sourced from the auto-ionization of water) is required to ionize H_2CO_3 in the $CO_2 – H_2O$ system.

Equation 4 describes a process with a high free energy barrier, the magnitude of which decreases with increasing availability of H_2O. Equation 4 could be written instead as:

$$nH_2O + CO_2 = H_2CO_3 + (n\text{-}1)H_2O \quad (8)$$

Nguyen et al. (2008) found an energy barrier of ~50 kcal / mol for n=1 decreasing to ~15 kcal / mol for n = 3. To more accurately reflect Equation 8, Equation 7 should be rewritten as:

$$nH_2O + CO_2 = H_3O^+ + HCO_3^- + (n\text{-}2)H_2O \quad (9)$$

Where n represents the two H_2O molecules consumed in the reaction plus molecules which assist in the formation of intermediary H_2CO_3. Additional H_2O is likely required to ionize H_2CO_3 and complex with H_3O^+. Neutral species such as H_2CO_3 are not detectable by conductivity measurements (although HCO_3^- and H_3O^+ would be detected), so our study cannot address the

extent to which non-ionized carbonic acid exists in dilute CO_2 – rich solutions. The free energy barrier to formation of carbonic acid in the absence of multiple 'helper' water molecules and the tendency of water to dissociate H_2CO_3 to neutral species (Tautermann, Voegele et al. 2002) suggests that CO_2 – H_2O solutions with low H_2O concentration may form little carbonic acid. If H_2CO_3 is formed in dilute solutions, it may not ionize to a significant extent due to low H_2O activity.

5 SUMMARY AND CONCLUSIONS

5.1 Summary

Across the entire range of CO_2 solutions examined, conductivity was below the estimated limit of quantification of 3.0 nS/cm at 1 kHz or ~9.5 nS/cm at infinite frequency. No detectable difference was observed between "dry" and "wet" CO_2, suggesting that the contribution due to ionization of H_2O (as H_2CO_3, by auto-ionization, or some other mechanism) was significantly less than the total conductivity. The conductivity of H_2O - CO_2 solutions in this study, ~ 1 – 9nS /cm at infinite frequency, are the same order of magnitude as the conductivity of paper, or at least 6 to 55 times less than the conductivity of ultra-pure (18.3 MΩ) water.

Assuming that conductivity measured was due only to the presence of H_2O (and subsequent formation and ionization of H_2CO_3), the conductivity is low, even when compared to an insulator such as ultra-pure conductivity water. The observed conductivity was comparable to that of nano-molal concentrations of ionized KCl in H_2O at 25°C and 1 bar. We therefore conclude that little or no ionization occurs in the bulk H_2O – CO_2 fluid across the range of temperatures, pressures, and compositions (CO_2 with up to ~1650 ppmw H_2O) tested in this study. At these conditions and concentrations, the bulk fluid does not form and/or ionize carbonic acid to any detectable extent.

In view of these results, we would suggest that bulk "wet" CO_2 is no more corrosive than "dry" CO_2. This result is in opposition to some other studies, such as (Lin, Fujii et al. 2008; McGrail, Schaef et al. 2009; Schaef, Windisch Jr et al. 2011) who provide evidence that minerals and metals in contact with "wet" CO_2 undergo rapid carbonization reactions. The concentrations

of H_2O tested in this study, < ~1650 ppmw H_2O, are less than the saturation concentrations at the conditions tested by Lin et al. (2008) and Schaef et al. (2011), but include concentrations that are saturated at the conditions tested by McGrail et al. (2009) (~25°C and 70 bar). We cannot rule out the possibility that ionization does occur in CO_2 with > ~1650 ppmw. However, our results clearly rule out significant ionization in the bulk fluid at H_2O saturation, 25°C and 80 bar. This H_2O concentration slightly exceeds saturation at ~25°C and 70 bar, conditions tested by McGrail et al. (2009), and suggests that ionization in the bulk fluid cannot explain the corrosion they reported. Our results support the conclusion reached by the aforementioned studies that these reactions are not due to ionization in the bulk fluid, and we confirm this conclusion for H_2O concentrations < ~1650 ppmw. Thus, the assumption that uniform ionization occurs throughout the bulk fluid (Fig. 1A) is not supported. A gradient in ionization as a function of distance from the substrate surface (Fig. 1B) cannot be excluded by our results if the region with significant ionization is small. For example, the carbonization reactions that occur under these conditions may be mediated by a thin film of aqueous fluid (Lin, Fujii et al. 2008) in which carbonic acid can form and ionize. Alternatively, these reactions may proceed due to direct molecular interaction of H_2O and CO_2 with some materials (Schaef, Windisch Jr et al. 2011), or have some other as yet unidentified cause.

5.2 Implications for enhanced geothermal energy production and CO_2 sequestration

Results of this study show that ionization in the bulk fluid, illustrated in Figure 1A, can be ruled out as a cause of the rapid corrosion and carbonation reactions that have been reported. This has implications for geoengineered system, such as enhanced geothermal energy production

using CO_2 as the working fluid and CO_2 sequestration in geologic formations, as well as other natural systems. Additional studies are recommended to determine if, and to what extent, thin films of aqueous fluids are responsible for these reactions and to what extent direct molecular interaction between the fluid and material surfaces are responsible. A better understanding of the mechanism(s) leading to corrosion of metal may lead to the development of processes to minimize corrosion and extend the lifetime of steel (and other materials) in contact with "wet" CO_2, reducing costs associated with enhanced geothermal energy production.

In a CO_2 storage reservoir, lack of ionization in the bulk fluid suggests that "wet" CO_2 may have little ability to transport inorganic ions over the range of temperatures and pressures tested (although geothermal systems may involve fluids at higher temperatures and pressures than those considered here). If this is the case, we should expect that formation of carbonate minerals will only occur at the site of the solid reactant(s) and will not occur at other locations via advective transport of dissolved components. Therefore, $CO_2 – H_2O$ – mineral reactions occurring in the cap rock of a CO_2 storage formation may enhance storage security. Reactions occurring in-place will not dissolve and transport material away from the site of reaction (with the exception of nonionic solutes, e.g. hydrocarbons). The positive change in volume resulting from the addition of "carbon" to the rock may decrease porosity and close fractures, giving the system a "self-healing" quality. This also suggests that $CO_2 – H_2O$ – mineral reactions with the host formation will tend to decrease permeability, which will in turn affect fluid flow through formations associated with CO_2 sequestration and enhanced geothermal energy production.

REFERENCES

Benson, S. M. and D. R. Cole (2008). "CO_2 Sequestration in Deep Sedimentary Formations." Elements **4**(5): 325-331.

Bockris, J. O., A. K. N. Reddy, et al. (2000). Fundamentals of Electrodics. New York, Kluwer Academic / Plenum Publishers.

Gaus, I. (2010). "Role and impact of CO_2-rock interactions during CO_2 storage in sedimentary rocks." International Journal of Greenhouse Gas Control **4**(1): 73-89.

Gaus, I., M. Azaroual, et al. (2005). "Reactive transport modelling of the impact of CO_2 injection on the clayey cap rock at Sleipner (North Sea)." Chemical Geology **217**(3-4): 319-337.

Intergovernmental Panel on Climate Change (2007). Climate Change 2007: Synthesis Report, Intergovernmental Panel on Climate Change.

Justice, J. C. (1983). Conductance of Electrolyte Solutions. Comprehensive Treatise of Electrochemistry. B. E. Conway, J. O. Bockris and E. Yeager. New York, Plenum Press. **5:** 223-337.

Lin, H., T. Fujii, et al. (2008). "Experimental evaluation of interactions in supercritical CO(2)/water/rock minerals system under geologic CO_2 sequestration conditions." Journal of Materials Science **43**(7): 2307-2315.

McGrail, B. P., H. T. Schaef, et al. (2009). "Water Reactivity in the Liquid and Supercritical CO2 Phase: Has Half the Story Been Neglected?" Energy Procedia **1**: 3415-3419.

Nguyen, M. T., M. H. Matus, et al. (2008). "Mechanism of the Hydration of Carbon Dioxide: Direct Participation of H_2O versus Microsolvation." Journal of Physical Chemistry A **112**(41): 10386-10398.

Pruess, K. (2006). "Enhanced geothermal systems (EGS) using CO_2 as working fluid - A novel approach for generating renewable energy with simultaneous sequestration of carbon." Geothermics **35**(4): 351-367.

Regnault, O., V. Lagneau, et al. (2009). "Experimental measurement of portlandite carbonation kinetics with supercritical CO_2." Chemical Geology **265**(1-2): 113-121.

Schaef, H. T., C. F. Windisch Jr, et al. (2011). "Brucite [$Mg(OH_2)$] carbonation in wet supercritical CO_2: An in situ high pressure X-ray diffraction study." Geochimica Et Cosmochimica Acta **75**(23): 7458-7471.

Tautermann, C. S., A. F. Voegele, et al. (2002). "Towards the experimental decomposition rate of carbonic acid (H_2CO_3) in aqueous solution." Chemistry-a European Journal **8**(1): 66-73.

Zimmerman, G. H. (1994). A Flow-through electrical conductance instrument for dilute aqueous solutions: Measurements of 1:1 electrolytes to 656 K and 28 MPa. Department of Chemistry and Biochemistry. Newark, Delaware, University of Delaware.

Zimmerman, G. H., M. S. Gruszkiewicz, et al. (1995). "New Apparatus for Conductance Measurements at High-Temperatures - Conductance of Aqueous-Solutions of LiCl, NaCl, NaBr, and CsBr at 28 MPa and Water Densities from 700 to 264 kg/ M(-3)." Journal of Physical Chemistry **99**(29): 11612-11625.